*Article*

Transactions of the Institute of Measurement and Control
35(8) 1139–1151

DOI: 10.1177/0142331213490597
tim.sagepub.com
SAGE

# Adaptive optimal control allocation using Lagrangian neural networks for stability control of a 4WS–4WD electric vehicle

**Murat Demirci[1] and Metin Gokasan[2]**

**Abstract**

This study involves a layered vehicle dynamics control system, which is composed of an adaptive optimal control allocation method using Lagrangian neural networks for optimal distribution of tyre forces and the sliding mode yaw moment observer for robust control of yaw dynamics. The proposed optimal control allocation method eliminates the requirement of solving optimization problem in every time step and it is a convergent and stability guaranteed solution for the optimal tyre force distribution problem. The aim in the sliding mode yaw moment observer is to force the vehicle to track a reference vehicle dynamic behaviour by estimating the equivalent input extended disturbance, which is the required stabilizing virtual yaw moment. The proposed layered stability control scheme has been tested on a four-wheel drive–four-wheel steer electric Fiat Doblo Van, which is modelled in CarSim. Both the sliding mode disturbance observer and the optimal control allocation methods are the first known applications to the stability control problem of road vehicles.

**Keywords**

Lagrangian neural networks, optimal control allocation, sliding mode control, vehicle dynamics control, yaw moment observer

## Introduction

In layered vehicle stability control systems, the upper layer is a yaw moment controller whose output is the virtual yaw moment control input to be generated by the middle and lower layers. While the middle layer deals with control allocation and produces actuator reference commands, servo controllers in the lower layer make the actuators track these reference values. The general requirements of a layered vehicle stability control system are: 1) a robust yaw moment controller, which is robust against modelling and parameter uncertainties of the vehicle, in addition to external yaw disturbances caused by side wind, $\mu$-split braking, etc., should be designed. (2) The vehicle actuators, like steering actuators, tractions motors, braking actuators, etc. to generate the required stabilizing yaw moment should be allocated in an optimal manner. (3) The control allocation problem should include vehicle dynamic limitations (tyre friction circle limitation, road adhesion, etc.) and actuator limitations. (4) The stability of the vehicle dynamics control system should be guaranteed and hence, a convergent and stability guaranteed optimal control allocation approach is required. (5) The challenge of solving the control allocation problem in every time step due to high computational efforts should be addressed.

Goodarzi and Esmailzadeh (2007) have developed a multilayer-type of vehicle dynamics control system in which a motion controller is designed based on optimal control theory to generate the required yaw moment for lateral motion of the vehicle and traction force for longitudinal motion. An analytical solution with fuzzy parameter adaptation is derived for tyre reference slip distribution and a sliding mode controller is used to control tyre slip. Geng et al. (2009) have proposed a direct yaw moment controller based on linear quadratic regulator (LQR) theory and an optimal in-wheel motor driving/braking force distributor. A fuzzy yaw moment controller and a fuzzy torque allocation algorithm have been developed by Feiqianq et al. (2009). Tahami et al. (2003) have combined the upper and middle layers and constructed a fuzzy logic-based yaw stability control system whose output is the required torque change of in-wheel motors. The required torque change is symmetrically distributed to create yaw moment difference. The authors do not take into account the saturation limits of the in-wheel motor torques. Moreover, the in-wheel motor torque distribution is very simple and not optimal. Anwar (2005) has designed a generalized predictive controller for yaw dynamics in the upper layer. The allocation of dictated yaw moment is achieved by using a heuristic torque distribution strategy for each electromagnetic brake at each wheel.

[1]TUBITAK Marmara Research Center, Energy Institute
[2]Istanbul Technical University, Control Engineering

**Corresponding author:**
Murat Demirci, TUBITAK MRC, TUBITAK Gebze Yerleskesi PK:21, Gebze, 41470, Turkey.
Email: Murat.Demirci@itu.edu.tr

Piyabongkarn at al. (2007) have studied the use of torque biasing devices, i.e. electronically controlled limited slip differential (ELSD) and centre coupler. They use a proportional controller to control yaw rate and heuristic decision logic to activate the ELSD or centre coupler.

The control allocation term refers to the distribution of the virtual yaw moment control input among the available actuators of the vehicle, e.g. front and rear wheel active steering actuators, mechanical braking actuators, electric motors, etc. Efficient, stable and convergent optimization techniques for optimal control allocation and robust control methods for servo control loops are crucial in the layered stability control systems. Mokhiamar and Abe (2006) have derived an optimization problem for optimal distribution of tyre forces in which the square sum of workloads of four wheels are taken as a cost function to be minimized. To simplify the optimization problem, they have converted the optimization problem into a linear equation system and it is solved in every time step. They have taken into account the tyre friction circle or tyre workload in the cost function but, since the friction circle limitation is not considered as an explicit non-linear inequality constraint to assure tyre forces in the friction circle, the solutions of the optimization algorithm may not be feasible. Moreover, the authors also have not taken into account the actuator limitations in the optimization problem. Cho at al. (2008) have proposed an optimal tyre force distribution method in which the friction circle limitation has been taken as a non-linear inequality constraint for integrating active front steering and a conventional electronic stability control system. They have derived an analytical solution for optimal tyre forces by solving the optimization problem using the Lagrange multipliers theory. Since they make some assumptions between lateral and longitudinal tyre forces to simplify the optimization problem and to find an analytical solution, the results are not optimal. Moreover, the actuator constraints are not considered in the problem so that the actuators may saturate and the dictated yaw moment cannot be produced by the actuators. Wang and Longoria (2009) have proposed a numerical optimization method called the accelerated fixed-point algorithm to solve the control allocation problem in which tyre slip and slip angles are chosen as allocation variables instead of tyre forces to simplify the optimization problem and to avoid the non-linear friction circle limitation of tyre forces. Plumlee et al. (2006) have studied a quadratic programming-based control allocation for distribution of front/rear-wheel steering angles and longitudinal tyre forces. Zhao and Zhang (2009) have used sequential dynamic programming approach for distribution of longitudinal tyre forces in a wheel-motored electric vehicle. Ono et al. (2006) have also proposed a sequential dynamic programming approach for tyre force distribution in a four-wheel distributed steering and four-wheel distributed traction/braking systems. Tyre grip margin and friction circle of each tyre are estimated and used in the tyre force distribution algorithm. Tjonnas and Johansen (2010) have proposed an adaptive control allocation method for the active steering and brake allocation problem. The allocation variables are tyre slip and steering angles.

If the control allocation includes a non-linear optimization problem, it is difficult to find an analytical solution and numerical optimization methods are used in the literature. However, the stability of the optimal control allocation should be guaranteed in a vehicle safety system and there is no an explicit way to show the stability of a numerical optimization method. Moreover, the numerical optimization-based control allocation requires the non-linear optimization problem to be solved in every time step for every corresponding virtual yaw moment input and this requires high computational effort in real-time implementation. To tackle these problems, this work proposes a Lagrangian neural network approach to solve the non-linear optimization problem adaptively, which avoids the requirement of solving the optimization problem explicitly in every time step, and the convergence and stability of the control allocation are guaranteed. The optimization problem is handled by Lagrange multipliers theory.

Another contribution of this work is the sliding mode yaw moment observer for yaw moment control, which bases the disturbance observer scheme proposed by Abidi and Sabanovic (2007). The aim in the sliding mode yaw moment observer is to force the vehicle to track a reference vehicle dynamic behaviour by estimating the equivalent input extended disturbance, which is the required stabilizing yaw moment. The equivalent input extended-disturbance term refers to estimation of the extended disturbance in control input side. The disturbance includes modelling and parameter uncertainties of the vehicle in addition to external yaw disturbances caused by side wind, yaw disturbance moment, etc.

The proposed algorithms have been tested on a four-wheel drive–four-wheel steer (4WD–4WS) electric Fiat Doblo Van, which is modelled in CarSim. The main contributions of the paper are: 1) a sliding mode yaw moment observer has been developed for yaw moment control problem and it is the first known application to the yaw moment control. On the other hand, the proposed sliding mode disturbance observer is a chattering-free approach while the conventional sliding mode yaw moment controllers, which have been proposed in the literature, include chattering in the control signal. (2) An adaptive optimal control allocation approach has been proposed as a novel control allocation scheme to solve the tyre force distribution problem adaptively. The proposed control allocation scheme avoids the requirement of solving the optimization problem explicitly in every time step. Moreover, the convergence and stability of the control allocation are guaranteed. (3) The proposed adaptive optimal control allocation scheme is a very useful method and can be extended to other control allocation problems that exist in flight controllers, power source allocation, etc.

## Vehicle dynamics control

The proposed vehicle dynamics control scheme is composed of three layers (Figure 1):

- *Upper layer* – the sliding mode yaw moment observer exists in this layer. Yaw rate and side slip angle are the controlled states and virtual yaw moment is the output of the yaw moment observer. It is aimed to force the vehicle to track a reference vehicle dynamic behaviour by

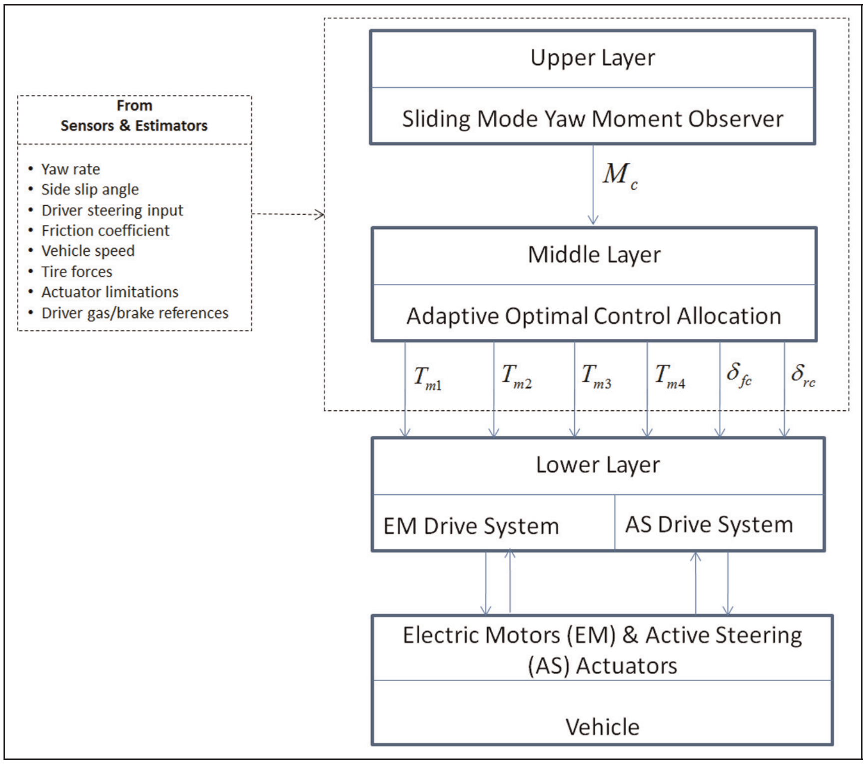


**Figure 1.** Layered vehicle dynamics control diagram.

estimating the equivalent input extended disturbance, which is the required stabilizing yaw moment. The reference vehicle dynamics are generated using linear two degree-of-freedom vehicle dynamics. Road friction coefficient, longitudinal vehicle speed and driver steering input information are used in the reference vehicle dynamics. Driver steering input and yaw rate can be measured by using dedicated low cost sensors but the measurement of side slip angle and road friction coefficient requires high-cost sensors, which are not affordable for a stability control system in road vehicles. Since the vehicle is driven by four electric motors mounted in wheels, it is not suitable to derive the vehicle speed information from wheel speed sensors, so the vehicle speed should be directly measured or estimated. Numerous estimation techniques have been proposed for estimation of side slip angle, road friction coefficient and vehicle speed in the literature, e.g. Han and Huh (2011), Anderson and Bevly (2010), Cheli et al. (2007), Stephant et al. (2007) and Piyabongkarn et al. (2009).

- *Middle layer* – this layer deals with optimal distribution of the virtual yaw moment reference dictated by the upper layer. The reference virtual yaw moment are generated by six actuators, which are four electric motors mounted in wheels, and front- and rear-wheel steering actuators. Optimal electrical motor torques and steering correction angles are calculated by solving a non-linear optimization problem, which includes a yaw moment equality constraint, the actuator and tyre force inequality constraints, and a cost function of adaptive weighted square sum of the tyre forces. The optimization problem is solved adaptively by using a Lagrangian neural network approach.
- *Lower layer* – this layer includes the electric motor drive system and active steering drive systems. Servo control loops for reference electric motor torques and steering angles calculated by the middle layer are included in the drive systems. Since the scope of this work does not include the lower layer actuator control, it is assumed here that all of the servo control loops are well tuned and the reference values are successfully tracked by the actuators.

## *Vehicle dynamics for controller design*

The vehicle dynamics

$$\begin{bmatrix} \dot{V}_{COG} \\ \dot{\beta} \\ \dot{r} \end{bmatrix} = -\begin{bmatrix} 0 \\ r \\ 0 \end{bmatrix} + \begin{bmatrix} \frac{1}{m}\cos\beta & \frac{1}{m}\sin\beta & 0 \\ -\frac{1}{mV_{COG}}\sin\beta & \frac{1}{mV_{COG}}\cos\beta & 0 \\ 0 & 0 & \frac{1}{I_Z} \end{bmatrix} \begin{bmatrix} \sum F_X \\ \sum F_Y \\ \sum M \end{bmatrix} \tag{1}$$

are two-track vehicle dynamics model that can be found in Kiencke and Nielsen (2005). The total tyre forces and yaw moment are defined as follows.

$$\begin{bmatrix} \sum F_x \\ \sum F_y \end{bmatrix} = \sum_{i=1}^{4} \begin{bmatrix} \cos\delta_i & -\sin\delta_i \\ \sin\delta_i & \cos\delta_i \end{bmatrix} \begin{bmatrix} F_{xi} \\ F_{yi} \end{bmatrix} - \begin{bmatrix} F_{xaero} + mg\sin\theta \\ 0 \end{bmatrix} \tag{2}$$

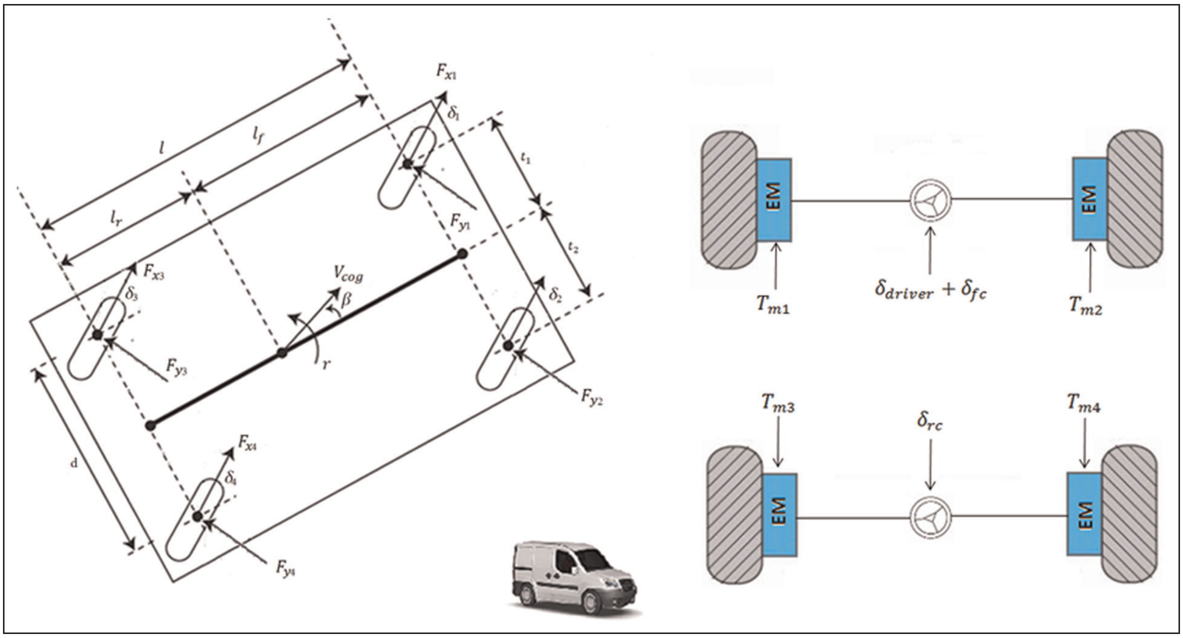


**Figure 2.** Vehicle diagrams.

$$\sum M = \sum_{i=1}^{4} \{ (F_{xi} \sin \delta_i + F_{yi} \cos \delta_i) l_{yi} + (-F_{xi} \cos \delta_i + F_{yi} \sin \delta_i) l_{xi} \} \tag{3}$$

The vehicle diagram is illustrated in Figure 2. The above non-linear two-track vehicle model can be reduced to the following linear single track model for small body side slip angle $\boldsymbol{\beta}$ and constant vehicle body speed $\boldsymbol{V_{COG}}$ over a limited time range by neglecting inclination and wind forces and assuming there is no difference between the left and right track ($\delta_1 = \delta_2 = \delta_f$, $\delta_3 = \delta_4 = \delta_r$).

$$\begin{bmatrix} \dot{\beta} \\ \dot{r} \end{bmatrix} = \begin{bmatrix} a_{11} & a_{12} \\ a_{21} & a_{22} \end{bmatrix} \begin{bmatrix} \beta \\ r \end{bmatrix} + \begin{bmatrix} b_{11} & b_{12} \\ b_{21} & b_{22} \end{bmatrix} \begin{bmatrix} \delta_f \\ \delta_r \end{bmatrix} + \begin{bmatrix} 0 \\ b_{23} \end{bmatrix} M_z \tag{4}$$

with

$$a_{11} = -\frac{2(C_f + C_r)}{mV_{COG}}, a_{12} = -1 - \frac{2(C_f l_f - C_r l_r)}{mV_{COG}^2}, \\ a_{21} = -\frac{2(C_f l_f - C_r l_r)}{I_z},$$

$$a_{22} = -\frac{2(C_f l_f^2 + C_r l_r^2)}{I_z V_{COG}}, b_{11} = \frac{2C_f}{mV_{COG}}, b_{12} = \frac{2C_r}{mV_{COG}}, \\ b_{21} = \frac{2C_f l_f}{I_z}, b_{22} = -\frac{2C_r l_r}{I_z}, b_{23} = \frac{1}{I_z}$$

Here, $M_z$ is called virtual yaw moment control input, which is derived for yaw moment manipulation from Equation (3) and defined as follows.

$$M_z = \sum_{i=1}^{4} \{ (\Delta F_{xi} \sin \delta_i + \Delta F_{yi} \cos \delta_i) l_{yi} \\ + (-\Delta F_{xi} \cos \delta_i + \Delta F_{yi} \sin \delta_i) l_{xi} \} \tag{5}$$

For small tyre steering angles, the trigonometric functions can be approximated as $\sin \delta_i \approx 0$ and $\cos \delta_i \approx 1$

$$M_z = \sum_{i=1}^{4} \Delta F_{yi} l_{yi} - \Delta F_{xi} l_{xi} \tag{6}$$

where $l_{x1} = l_{x3} = t_1$, $l_{x2} = l_{x4} = -t_2$, $l_{y1} = l_{y2} = l_f$ and $l_{y3} = l_{y4} = l_r$.

## Sliding mode yaw moment observer

The aim in the sliding mode yaw moment observer is to force the vehicle to track a reference two degree-of-freedom vehicle dynamic behaviour by estimating the equivalent input extended disturbance, which is the required stabilizing yaw moment. In order to generate the reference vehicle dynamics, the steady-state gains of the side slip angle and yaw rate dynamics in Equation (4) are considered and the following first-order reference vehicle dynamics are used in this work.

$$\dot{x}_d = A_d x_d + B_d M_d \tag{7}$$

with

$$A_d = \begin{bmatrix} \frac{-1}{\tau_d} & 0 \\ 0 & \frac{-1}{\tau_d} \end{bmatrix}, B_d = \begin{bmatrix} \frac{K_t}{\tau_d} \\ \frac{K_m}{\tau_d} \end{bmatrix}, x_d = \begin{bmatrix} \beta_d \\ r_d \end{bmatrix}, M_d = \frac{K_s}{K_m} \delta_f$$

where $r_d$ and $\beta_d$ are the yaw rate and vehicle side slip angle references repectively, $K_s$, $K_t$ and $K_m$ are input gains, $M_d$ is desired virtual yaw moment input and $\tau_d$ is time constant, which are defined as follows:

$$K_t = \frac{b_{23} a_{12}}{a_{11} a_{22} - a_{21} a_{12}}, \quad K_m = \frac{b_{23} a_{11}}{a_{21} a_{12} - a_{11} a_{22}},$$

$$K_s = \frac{b_{11}a_{21} - b_{21}a_{11}}{a_{11}a_{22} - a_{21}a_{12}}, \tau_d = \frac{b_{11}a_{21} - b_{21}a_{11}}{b_{21}(a_{11}a_{22} - a_{21}a_{12})} \quad (8)$$

The above desired reference yaw rate and side slip angle dynamics cannot always be obtained. It is not safe to try and obtain the desired reference dynamics if the road friction coefficient is unable to provide the forces to support high yaw rate and side slip angle dynamics. Hence, the reference yaw rate and side slip angle dynamics are limited as follows (Rajamani, 2006).

$$r_d \leqslant 0.85 \frac{\mu g}{V_{COG}} \quad (9)$$

$$\beta_d \leqslant \tan^{-1} \mu g \quad (10)$$

where $\mu$ is the road friction coefficient and $g$ is the acceleration of gravity.

Vehicle speed-dependent implementation of the reference vehicle dynamics is considered in this work. The input gains and the time constant defined in (8) depend on vehicle speed. The dependence of the reference vehicle dynamics on vehicle speed makes the controller speed-scheduled and the scheduling allows the controller to track a true reference vehicle dynamics (Aksun Guvenc et al., 2009).

The vehicle dynamics can be written as follows in terms of the reference dynamics.

$$\begin{gathered} \dot{x} = (A_d + \Delta A)x + (B_d + \Delta B)M_z + n \\ y = Cx \end{gathered} \quad (11)$$

where $x = [\beta \quad r]$ is state vector, $y$ is output vector, $\Delta A$ and $\Delta B$ are state and input matrix uncertainties and $n$ is modelling and parameter uncertainties and external disturbances. If an extended disturbance term, $N$ is defined as

$$N = \Delta A x + \Delta B M_z + n \quad (12)$$

and under the condition that there exists an equivalent input extended disturbance (EIED), $M_{ze}$ in the control input channel, the extended disturbance can be written as

$$N = B_d M_{ze} \quad (13)$$

It is shown by She et al. (2007) that if $(A_d, B_d, C)$ is observable and controllable and $(A_d, B_d, C)$ has no zeros on the imaginary axis, then there always exists an EIED in the control input channnel. Substituting Equations (12) and (13) into (11) yields

$$\dot{x} = A_d x + B_d(M_z + M_{ze}) \quad (14)$$

Then, by adapting the observer scheme proposed by Abidi and Sabanovic (2007), the disturbance observer is of the following form

$$\dot{\hat{x}} = A_d \hat{x} + B_d(M_z - M_c) \quad (15)$$

where $M_c$ is the observer control input. The following sliding surface, $\sigma$

$$\sigma = \Gamma(\hat{x} - x), \Gamma > 0 \quad (16)$$

and Lyapunov function, $V$

$$V = \frac{1}{2}\sigma^2 \quad (17)$$

are selected to design the disturbance observer based on sliding mode control theory. To satisfy Lyapunov stability criteria,

$$\begin{gathered} \dot{V} = \sigma\dot{\sigma} < 0 \\ \sigma\dot{\sigma} = -D\sigma^2, D > 0 \end{gathered} \quad (18)$$

is chosen. Then, the sliding surface dynamic is achieved as

$$\dot{\sigma} + D\sigma = 0 \quad (19)$$

Derivative of the sliding surface is

$$\dot{\sigma} = \Gamma(\dot{\hat{x}} - \dot{x}) \quad (20)$$

By using Equations (14) and (15), Equation (20) can be written as follows.

$$\begin{gathered} \Gamma(\dot{\hat{x}} - \dot{x}) + D(\hat{x} - x) = 0 \\ \Gamma A_d(\hat{x} - x) - \Gamma B_d(M_c + M_{ze}) + D(\hat{x} - x) = 0 \end{gathered} \quad (21)$$

Then, the observer control input is

$$M_c = -M_{ze} + (\Gamma B_d)^{-1}(\Gamma A_d + D)(\hat{x} - x) \quad (22)$$

If Equation (22) is examined, it can be seen that

$$\sigma \to 0 \Rightarrow x \to \hat{x} \Rightarrow M_c \to -M_{ze} \quad (23)$$

On the other hand, the derivative of the sliding surface can be written as

$$\dot{\sigma} = \Gamma A_d(\hat{x} - x) - \Gamma B_d(M_c + M_{ze}) \quad (24)$$

Then, an equivalent control input, $M_{ce}$ which makes $\dot{\sigma} = 0$, is found as

$$\dot{\sigma} = 0 \Rightarrow M_{ce} = B_d^{-1} A_d(\hat{x} - x) - M_{ze} \quad (25)$$

Substituting $M_{ce}$ in Equation (25) into Equations (24) and (19) yields

$$\begin{gathered} \dot{\sigma} = \Gamma B_d(M_{ce} - M_c) \\ \Gamma B_d(M_{ce} - M_c) + D\sigma = 0 \end{gathered} \quad (26)$$

Discretizing Equation (26) yields

$$\begin{gathered} \frac{\sigma(k) - \sigma(k-1)}{T} = \Gamma B_d(M_{ce}(k-1) - M_c(k-1)) \\ \Gamma B_d(M_{ce}(k) - M_c(k)) + D\sigma(k) = 0 \end{gathered} \quad (27)$$

where $T$ is sampling time and $k$ is index term. If the equivalent control inputs are extracted in (27) as

$$M_{ce}(k) = M_c(k) - (\Gamma B_d)^{-1} D\sigma(k)$$

$$M_{ce}(k-1) = M_c(k-1) + (\Gamma B_d)^{-1}\left(\frac{\sigma(k)-\sigma(k-1)}{T}\right) \quad (28)$$

and by defining a relation between the control inputs as follows

$$M_{ce}(k) - M_{ce}(k-1) = P(M_{ce}(k-1) - M_c(k-1)),\ P > 0 \quad (29)$$

the sliding mode disturbance observer-based yaw moment controller of the following form is achieved.

$$M_c(k) = M_c(k-1) + K_c\left(D_c\sigma(k) + \frac{\sigma(k)-\sigma(k-1)}{T}\right) \quad (30)$$

where $K_c = P(\Gamma B_d)^{-1}$ and $D_c = \frac{D}{T}$.

## Adaptive optimal control allocation

Once the required yaw moment for stabilization of the vehicle is calculated using the sliding mode yaw moment observer given in the above chapter, the remaining tasks are to distribute the tyre forces optimally, which generate the required yaw moment, and to allocate the actuators. While distributing the tyre forces, the non-linear friction circle limitations of the tyre forces should be taken into account. The non-linear friction circle limitation is

$$(F_{xi})^2 + (F_{yi})^2 \leqslant (\mu_i F_{zi})^2 \quad (31)$$

For 4WD–4WS electric vehicles, front and rear wheel steering actuators and four electric motors mounted in wheels can be used for yaw moment generation. Actuator limitations should also be considered for a feasible control allocation. The limitations for steering actuators and electric motors are

$$-T_{mi\_max} \leqslant T_{mi} \leqslant T_{mi\_max} \quad (32)$$

$$-\delta_{i\_max} \leqslant \delta_i \leqslant \delta_{i\_max} \quad (33)$$

For mapping the tyre forces into real actuator control signals, i.e. $T_{mi}$ and $\delta_i$, wheel rotational dynamics and simple tyre model are considered. Since the wheel rotational dynamic is

$$J_{wi}\frac{d\omega_i}{dt} = T_{mi} - T_{bi} - F_{xi}R \quad (34)$$

the motor torques are changed as $\Delta T_{mi} = \Delta F_{xi}R$. In a same manner, for small tyre side slip angles, the tyre steering angle can be determined as

$$\delta_i \approx \left\{ \begin{array}{l} \beta + \frac{l_f r}{V_{COG}} + \alpha_i, i = 1,2 \\ \beta - \frac{l_r r}{V_{COG}} + \alpha_i, i = 3,4 \end{array} \right\} \quad (35)$$

where $\alpha_i \approx \frac{F_{yi}}{C_i}$, the tyre steering angle are changed as $\Delta\delta_i \approx \frac{\Delta F_{yi}}{C_i}$. Thus, for 4WD–4WS electric vehicles, the optimal tyre force distribution problem (OTFDP) is formulated as follows.

$$\min\ f(u) = \sum_{i=1}^{4} (\gamma_i \Delta F_{xi}^2 + \rho_i \Delta F_{yi}^2)$$

$$s.t \left\{ \begin{array}{c} h(u) = \sum_{i=1}^{4} (\Delta F_{yi} l_{yi} - \Delta F_{xi} l_{xi}) - M_c = 0 \\ (F_{xi} + \Delta F_{xi})^2 + (F_{yi} + \Delta F_{yi})^2 \leqslant (\mu_i F_{zi})^2 \\ -T_{mi\_max} \leqslant T_{mi} + \Delta F_{xi} R \leqslant T_{mi\_max} \\ -\delta_{i\_max} \leqslant \delta_i + \frac{\Delta F_{yi}}{C_i} \leqslant \delta_{i\_max} \end{array} \right. \quad (36)$$

where $u = \left[\Delta F_{x1}\Delta F_{x2}\Delta F_{x3}\Delta F_{x4}\Delta F_{y1}\Delta F_{y2}\Delta F_{y3}\Delta F_{y4}\right]^T$, $\gamma_i$ and $\rho_i$ are longitudinal and lateral weighting factors. By redefining the inequality constraints as

$$g(u) = \left\{ \begin{array}{c} (F_{xi} + \Delta F_{xi})^2 + (F_{yi} + \Delta F_{yi})^2 - (\mu_i F_{zi})^2 \leqslant 0 \\ -T_{mi\_max} - T_{mi} - \Delta F_{xi} R \leqslant 0 \\ T_{mi} + \Delta F_{xi} R - T_{mi\_max} \leqslant 0 \\ -\delta_{i\_max} - \delta_i - \frac{\Delta F_{yi}}{C_i} \leqslant 0 \\ \delta_i + \frac{\Delta F_{yi}}{C_i} - \delta_{i\_max} \leqslant 0 \end{array} \right\},$$

$$i = 1,2,3,4 \quad (37)$$

it can be seen that the optimization problem includes one equality and 20 inequality constraints. If the problem is formulated by well-known Lagrange Multiplier Theorem, the Lagrangian function becomes

$$L(u,\eta,\lambda,s) = f(u) + h(u).\lambda + \sum_{j=1}^{20} \eta_j (g_j(u) + s_j^2) \quad (38)$$

where $\lambda$ and $\eta_j$ are the Lagrangian multipliers and $s_j$ is slack variable. A Karush–Khun–Tucker (KKT) point of the optimization problem is defined as a point $(u^*, \eta^*, \lambda^*)$ satisfying the conditions below (Zhang and Constantinidis, 1992).

$$\nabla_u L(u^*,\eta^*,\lambda^*) = \frac{\partial f(u^*)}{\partial u_i} + \lambda^* \frac{\partial h(u^*)}{\partial u_i} + \sum_{j=1}^{20} \eta_j^* \frac{\partial g_j(u^*)}{\partial u_i} = 0 \quad (39a)$$

$$h(u^*) = 0 \quad (39b)$$

$$g_j(u^*) \leqslant 0 \quad (39c)$$

$$\eta_j^*.g_j(u^*) = 0 \quad (39d)$$

$$\eta_j^* \geqslant 0 \quad (39e)$$

If the gradients of equality and active inequality constraints are linearly independent and KKT conditions are hold, then $u^*$ is local minimum point of the optimization problem. Since OTFDP is a convex optimization problem, the point $u^*$ is also a global minimum point.

Since the OTFDP is a non-linear optimization problem and it is difficult to find an analytical solution, an adaptive dynamic system is proposed to find an optimal solution. The aim is to design a neural network that will always converge to a KKT point of the optimization problem. Such a neural network based on the MaxQ method is proposed by Wah and Wang (1999). The inequality constraints given in Equation (37) can be converted into equality constraints by using MaxQ method instead of the slack variable method. The MaxQ method eliminates the need for slack variables and decreases the dimension of the problem. Hence, the Lagrangian function of the MaxQ method becomes

$$L(u,\eta,\lambda) = f(u) + h(u).\lambda + \sum\nolimits_{j=1}^{20} \eta_j p_j(u) \tag{40}$$

where

$$p_j(u) = \max\big(0, g_j(u)\big) \tag{41}$$

It has been shown by Wah and Wang (1999) that the stationary point of the following adaptive dynamic system is a KKT point of the optimization problem and the stationary point will be converged if the stationary point is asymptotically stable and the adaptive dynamic system is globally Lyapunov stable.

$$\frac{du}{dt} = -K_u \frac{\partial L(u,\eta,\lambda)}{\partial u} \tag{42a}$$

$$\frac{d\lambda}{dt} = K_\lambda \frac{\partial L(u,\eta,\lambda)}{\partial \lambda} = K_\lambda h(u) \tag{42b}$$

$$\frac{d\eta}{dt} = K_\eta \frac{\partial L(u,\eta,\lambda)}{\partial \eta} = K_\eta p(u) \tag{42c}$$

where $K_u \in \mathbb{R}^{8x8}$, $K_\lambda \in \mathbb{R}^1$ and $K_\eta \in \mathbb{R}^{20x20}$ are diagonal matrices, which determine convergence rates.

If the weighting coefficients, $\gamma_i$ and $\rho_i$ in the cost function are chosen by considering the tyre workload such as

$$\gamma_i = \left(\frac{\Delta F_{xi}}{\mu_i F_{zi}}\right)^2, i = 1,2,3,4 \tag{43a}$$

$$\rho_i = \left(\frac{\Delta F_{yi}}{\mu_i F_{zi}}\right)^2, i = 1,2,3,4 \tag{43b}$$

the optimal tyre forces can be determined by the following adaptive dynamic system.

$$\frac{d\Delta F_{xi}}{dt} = k_{fxi}\left(2\Delta F_{xi}\gamma_i + \frac{2}{(\mu_i F_{zi})^2}\Delta F_{xi}^3 - \lambda l_{xi} + 2\eta_i(F_{xi} + \Delta F_{xi}) + R(\eta_{i+4} - \eta_{i+8})\right) \tag{44a}$$

$$\frac{d\Delta F_{yi}}{dt} = k_{fyi}\left(2\Delta F_{yi}\rho_i + \frac{2}{(\mu_i F_{zi})^2}\Delta F_{yi}^3 + \lambda l_{yi} + 2\eta_i\big(F_{yi} + \Delta F_{yi}\big) + C_i^{-1}(\eta_{i+16} - \eta_{i+12})\right) \tag{44b}$$

$$\frac{d\eta_j}{dt} = k_{\eta j}\max\big(0, g_j(u)\big) \tag{44c}$$

$$\frac{d\lambda}{dt} = k_\lambda\left(\sum_{i=1}^{4}(\Delta F_{yi} l_{yi} - \Delta F_{xi} l_{xi}) - M_c\right) \tag{44d}$$

where $k_{fxi}$, $k_{fyi}$, $k_{\eta j}$ and $k_\lambda$ are the convergence gains, $i = 1,2,3,4$ and $j = 1,2,3,\ldots,20$. Convergence and stability proof of the proposed adaptive optimal control allocation method are given in the appendix.

Once the optimal tyre forces ($\Delta F_{xi}$, $\Delta F_{yi}$) are determined, the electric motor and steering actuator commands are calculated as

$$T_{mi} = \frac{T_{md}}{4} + R.\Delta F_{xi} \tag{45}$$

$$\delta_{fc} = \eta \cdot \left(\frac{\Delta F_{y1} + \Delta F_{y2}}{2 \cdot C_f}\right) \tag{46}$$

$$\delta_{rc} = \eta \cdot \left(\frac{\Delta F_{y3} + \Delta F_{y4}}{2 \cdot C_r}\right) \tag{47}$$

where $T_{md}$ is drive/brake input of the driver and $\eta$ is steering ratio.

## Application and simulation results

The proposed vehicle dynamics control approach has been tested on a 4WD–4WS electric Fiat Doblo Van (Figure 3), which is modelled in CarSim simulation software. The vehicle is equipped with four axle motors, and front and rear steering actuators. The vehicle dynamic control system is modelled in Matlab/Simulink and it is co-simulated with CarSim. The first test scenario is double lane-change (DLC) manoeuvre. In the DLC manoeuvre, a driver steering input as shown in Figure 4 and a fixed 20% throttle input have been applied to the vehicle with initial speeds of 130 and 120 km/h on a wet road and an icy road, respectively. The aim is to evaluate the performance of the proposed control approach in extreme driving manoeuvres in which the vehicle dynamics is highly non-


**Figure 3.** Fiat Doblo Van.

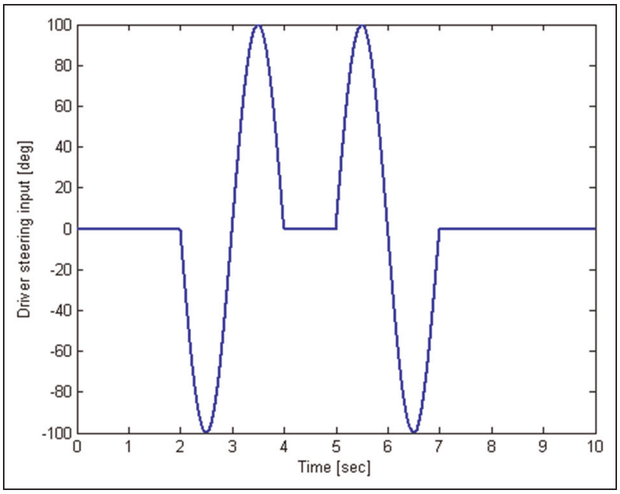


**Figure 4.** Driver steering input in double lane-change (DLC) manoeuvres.

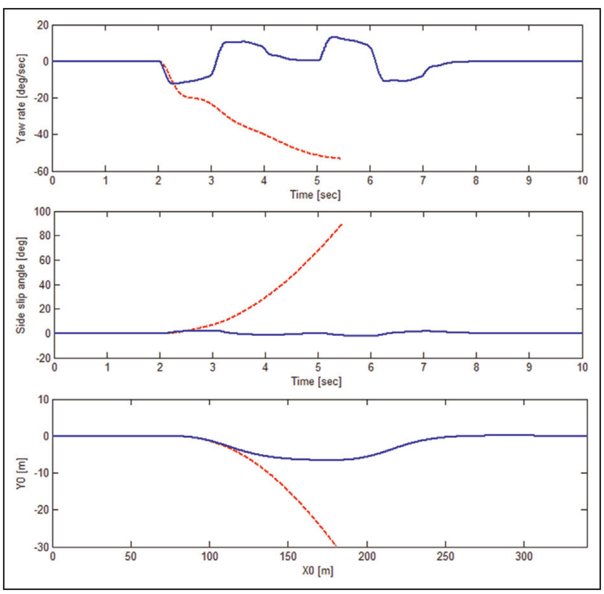


**Figure 5.** The obtained results in double lane-change (DLC) manoeuvre with initial speed of 130 km/h on a wet road (red-dot line: uncontrolled vehicle, blue-continuous line: controlled vehicle).

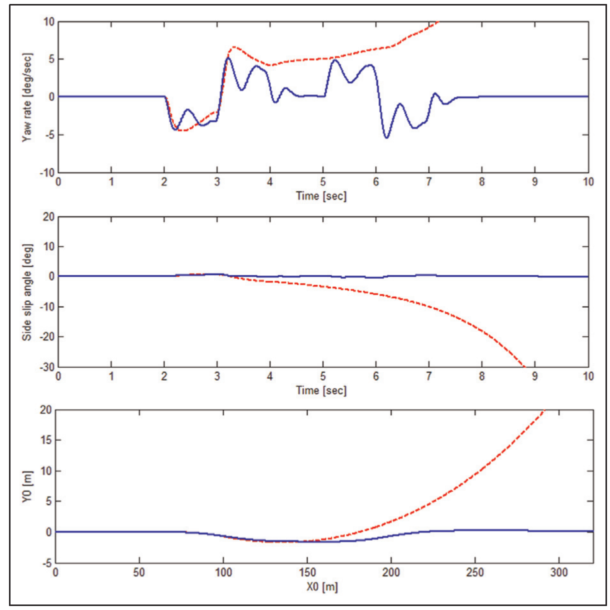


**Figure 6.** The obtained results in double lane-change (DLC) manoeuvre with initial speed of 120 km/h on an icy road (red-dot line: uncontrolled vehicle, blue-continuous line: controlled vehicle).

linear, and there are highly non-linear modelling and parameter uncertainties.

By examining Figures 5 and 6, it can be seen that the vehicle equipped with the proposed controller makes DLC manoeuvres successfully while the uncontrolled vehicle cannot and the vehicle drifts out. The control system is very successful in improving the handling and stability of the vehicle even in extreme driving manoeuvres. The actuator efforts that are allocated using the proposed adaptive optimal control allocation approach are given in Figures 7 and 8. The yaw moment is successfully distributed between the actuators in an optimal manner.

The other test scenario is a cross-wind disturbance rejection (CWDR) test in which the aim is to evaluate the performance of the proposed control system against external yaw disturbances. In this test, the vehicle enters in to a test track in which there exist fan blowers at each side and specific positions of an icy road to create a 100-km/h side wind. The initial speed of the vehicle is 120 km/h and 20% throttle input has been applied to the vehicle during the test. Figure 9 shows the obtained results of the yaw rate and the vehicle trajectories for uncontrolled and controlled cases. It can be seen that the proposed control system reject the effects of the wind disturbance in an effective way even on a low-friction road while the uncontrolled vehicle drifts out. The allocated actuator efforts are shown in Figure 10 (a) and (b).

## Conclusion

The paper has proposed adaptive optimal control allocation method for optimal tyre force distribution problem and sliding mode yaw moment observer for yaw moment control. Adaptive optimal control allocation method eliminates the requirement of solving optimization problem in every time step and it is a convergent and stability guaranteed solution for optimal tyre force distribution problem. The proposed method has been tested on a 4WD–4WS electric Fiat Doblo Van. The simulation results for DLC manoeuvre and CWDR test carried out in CarSim environment shows that the proposed control allocation approach is very successful in vehicle dynamic stabilization and optimal control allocation.

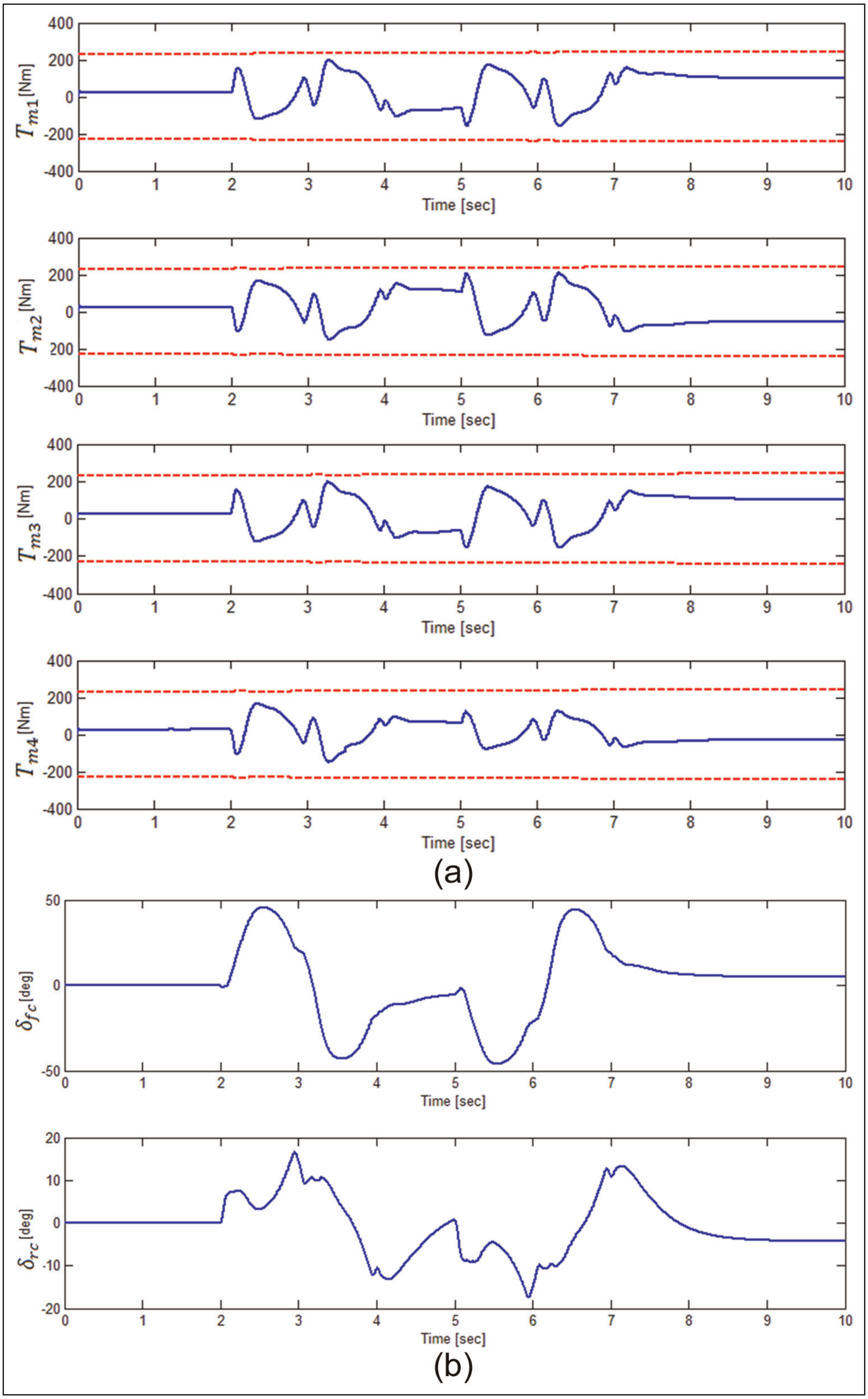


**Figure 7.** (a) The motor torques in double lane-change (DLC) manoeuvre with initial speed of 130 km/h on a wet road (red-dot lines shows the motor torque limits); (b) the steering angles in DLC manoeuvre with initial speed of 130 km/h on a wet road.

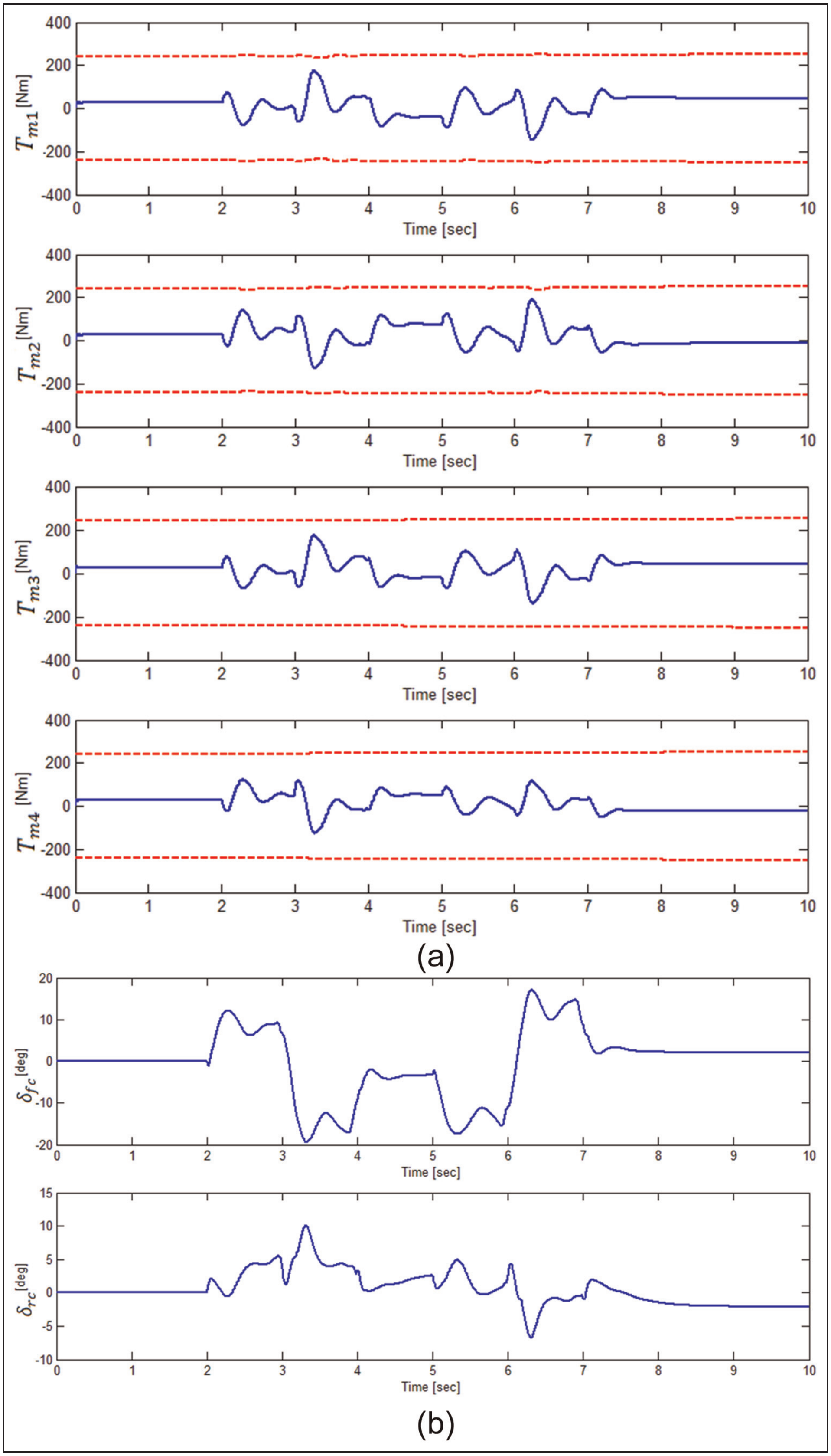


**Figure 8.** (a) The motor torques in double lane-change (DLC) manoeuvre with initial speed of 120 km/h on an icy road (red-dot lines shows the motor torque limits); (b) the steering angles in DLC manoeuvre with initial speed of 120 km/h on an icy road.

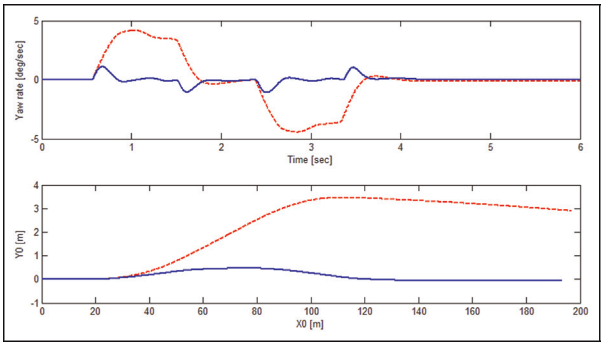


**Figure 9.** The obtained results for cross-wind disturbance rejection (CWDR) test (red-dot: uncontrolled vehicle, blue-continuous: controlled vehicle).

## References


Abidi K and Sabanovic A (2007) Sliding-mode control for high-precision motion of a piezostage. *IEEE Transactions on Industrial Electronics* 54(1): 629–637.

Aksun Guvenc B, Guvenc L and Karaman S (2009) Robust yaw stability controller design and hardware-in-the-loop testing for a road vehicle. *IEEE Transactions on Vehicular Technology* 58(2): 555–571.

Anderson R and Bevly MD (2010) Using GPS with a model based estimator to estimate critical vehicle states. *Vehicle System Dynamics* 48(12): 1413–1438.

Anwar S (2005) Yaw stability control of an automotive vehicle via generalized predictive algorithm. *Proceedings of the American Control Conference*, 435–440.


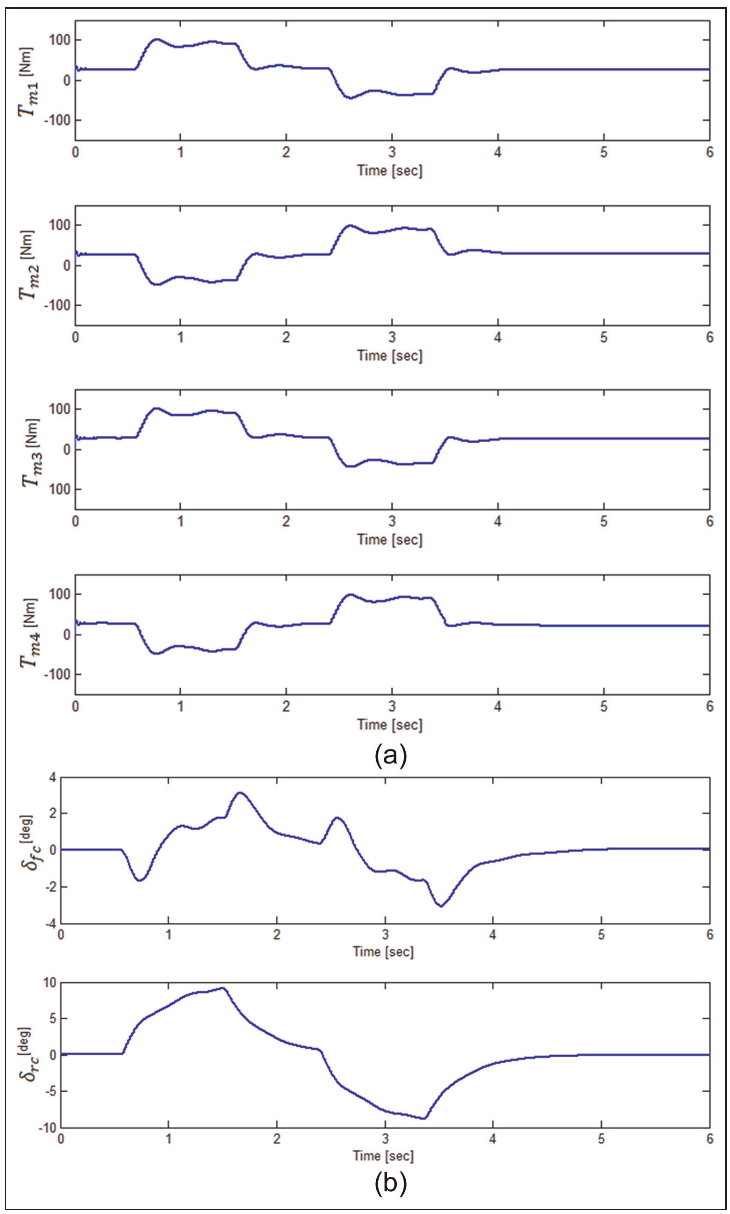


**Figure 10.** (a) The motor torques in cross-wind disturbance rejection (CWDR) test; (b) the steering angles in CWDR test.

Cheli F, Sabbiano E, Pesce M, et al. (2007) A methodology for vehicle side slip angle identification: comparison with experimental data. *Vehicle System Dynamics* 45(6): 549–563

Cho W, Yoon J, Kim J, et al. (2008) An investigation into unified chassis control scheme for optimised vehicle stability and manoeuvrability. *Vehicle System Dynamics* 46(Supplement): 87–105.

Feiqiang L, Jun W and Zhaodu L (2009), Motor torque based vehicle stability control for four-wheel-drive electric vehicle. *Proceedings of the IEEE Vehicle Power and Propulsion Conference*, 1596–1601.

Geng C, Mostefai L, Denai M, et al. (2009) Direct-yaw moment control of an in-wheel motored electric vehicle based on body slip angle fuzzy observer. *IEEE Transactions on Industrial Electronics* 56(5): 1411–1419.

Goodarzi A and Esmailzadeh E (2007) Design of a VDC system for all-wheel independent drive vehicles. *IEEE/ASME Transactions on Mechatronics* 12(6): 1413–1438.

Han S and Huh K (2011) Monitoring system design for lateral vehicle motion. *IEEE Transactions on Vehicular Technology* 60(4): 1394–1403.

Kiencke U and Nielsen L (2005) *Automotive Control Systems - For Engine, Driveline, and Vehicle*, 2nd ed. Germany: Springer.

Mokhiamar O and Abe M (2006) How the four wheels should share forces in an optimum cooperative chassis control. *Control Engineering Practice* 14(3): 295–304.

Ono E, Hattori Y, Muragishi Y, et al. (2006) Vehicle dynamics integrated control for four-wheel-distributed steering and four-wheel-distributed traction/braking systems. *Vehicle System Dynamics* 44(2): 139–151.

Piyabongkarn D, Lew JY, Rajamani R, et al. (2007) On the use of torque-biasing systems for electronic stability control: limitations and possibilities. *IEEE Transactions on Control Systems Technology* 15(3): 581–589.

Piyabongkarn D, Rajamani R, Grogg JA, et al. (2009) Development and experimental evaluation of a slip angle estimator for vehicle stability control. *IEEE Transactions on Control Systems Technology* 17(1): 78–88.

Plumlee JH, Bevly BM and Hodel AS (2006) Control allocation in ground vehicles. *International Journal of Vehicle Design* 42(3/4): 215–243.

Rajamani R (2006) *Vehicle Dynamics and Control*. USA: Springer.

She JH, Xin X and Ohyama Y (2007) Estimation of equivalent input disturbance improves vehicle steering control. *IEEE Transactions on Vehicular Technology* 56(6):3722–3731.

Stephant J, Chara A and Meizel D (2007) Evaluation of a sliding mode observer for vehicle side slip angle. *Control Engineering Practice* 15(7): 803–812.

Tahami F, Kazemi R and Farhanghi S (2003) A novel driver assist stability system for all wheel drive electric vehicles. *IEEE Transactions on Vehicular Technology* 53(3): 683–692.

Tjonnas J and Johansen TA (2010) Stabilization of automotive vehicles using active steering and adaptive brake control allocation. *IEEE Transactions on Control Systems Technology* 18(3): 545–558.

Wah WB and Wang T (1999) *Efficient and Adaptive Lagrange-Multiplier Methods for Nonlinear Continuous Global Optimization* 14(1): 1–25.

Wang J and Longoria RG (2009) Coordinated and reconfigurable vehicle dynamics control. *IEEE Transactions on Control Systems Technology* 17(3): 723–732.

Zhang S and Constantinides AG (1992), Lagrange Programming Neural Networks, *IEEE Transactions on Circuits and Systems-II: Analog and Digital Signal Processing* 39(7): 441–452.

Zhao Y and Zhang J (2009) Yaw stability control of a four-independent-wheel drive electric vehicle. *International Journal of Electric and Hybrid Vehicles* 2(1): 64–76.

## Appendix

To show the global stability of the proposed adaptive optimal control allocation method given in (42), a Lyapunov function, $V$ is defined as follows.

$$V(u,\lambda,\eta) = \frac{1}{2}\left(\left(\frac{\partial L}{\partial u}\right)^T K_u\left(\frac{\partial L}{\partial u}\right) + \left(\frac{\partial L}{\partial \eta}\right)^T K_\eta\left(\frac{\partial L}{\partial \eta}\right) + \left(\frac{\partial L}{\partial \lambda}\right)^T K_\lambda\left(\frac{\partial L}{\partial \lambda}\right)\right) \tag{A1}$$

Derivative of the Lyapunov function is

$$\frac{dV}{dt} = \frac{\partial V}{\partial u}\frac{du}{dt} + \frac{\partial V}{\partial \lambda}\frac{d\lambda}{dt} + \frac{\partial V}{\partial \eta}\frac{d\eta}{dt} \tag{A2}$$

$$\begin{aligned}\frac{dV}{dt} = &\left(\left(\frac{\partial L}{\partial u}\right)^T K_u\left(\frac{\partial^2 L}{\partial u^2}\right) + \left(\frac{\partial L}{\partial \eta}\right)^T K_\eta\left(\frac{\partial^2 L}{\partial \eta^2}\right)\right.\\ &\left.+ \left(\frac{\partial L}{\partial \lambda}\right)^T K_\lambda\left(\frac{\partial^2 L}{\partial \lambda^2}\right)\right)\frac{du}{dt} + \left(\left(\frac{\partial L}{\partial u}\right)^T K_u\left(\frac{\partial^2 L}{\partial u\partial \lambda}\right)\right)\frac{d\lambda}{dt}\\ &+ \left(\left(\frac{\partial L}{\partial u}\right)^T K_u\left(\frac{\partial^2 L}{\partial u\partial \eta}\right)\right)\frac{d\eta}{dt}\end{aligned} \tag{A3}$$

By substituting Equation (42) in to (A3), one can achieve

$$\begin{aligned}\frac{dV}{dt} &= -\left(\frac{\partial L}{\partial u}\right)^T K_u\left(\frac{\partial^2 L}{\partial u^2}\right)K_u\left(\frac{\partial L}{\partial u}\right)\\ &= -\left(\frac{\partial L}{\partial u}\right)^T K_u\ diag\left\{\frac{\partial^2 L}{\partial \Delta F_{xi}^2}, \frac{\partial^2 L}{\partial \Delta F_{yi}^2}\right\}K_u\left(\frac{\partial L}{\partial u}\right)\end{aligned} \tag{A4}$$

Since

$$\frac{\partial^2 L}{\partial \Delta F_{xi}^2} > 0, \frac{\partial^2 L}{\partial \Delta F_{yi}^2} > 0, i = 1,2,3,4 \tag{A5}$$

the derivative of the Lyapunov function is negative,

$$\frac{dV}{dt} < 0 \tag{A6}$$

Hence $V(u,\lambda,\eta)$, is a Lyapunov function for the system and the proposed adaptive optimal control allocation scheme is Lyapunov stable.

On the other hand, let us consider linearizing first-order equations in (42) at the equilibrium point $(u^*,\lambda^*,\eta^*)$. The local characteristic of the equilibrium is determined by the linearized system. The linearized system is

$$\begin{bmatrix} \frac{du}{dt} \\ \frac{d\lambda}{dt} \\ \frac{d\eta}{dt} \end{bmatrix} = -\underbrace{\begin{bmatrix} K_u & 0 & 0 \\ 0 & K_\lambda & 0 \\ 0 & 0 & K_\eta \end{bmatrix}}_{K} \underbrace{\begin{bmatrix} \frac{\partial^2 L}{\partial u^2} & \frac{\partial^2 L}{\partial u \partial \lambda} & \frac{\partial^2 L}{\partial u \partial \eta} \\ -\frac{\partial^2 L}{\partial \lambda \partial u} & 0 & 0 \\ -\frac{\partial^2 L}{\partial \eta \partial u} & 0 & 0 \end{bmatrix}}_{G} \begin{bmatrix} u - u^* \\ \lambda - \lambda^* \\ \eta - \eta^* \end{bmatrix} \quad \text{(A7)}$$

Since $K > 0$, if the real part of the each eigenvalue of $G$ is strictly positive, $(u^*, \lambda^*, \eta^*)$ is asymptotically stable point of the system. Assuming $[\hat{x} \quad \hat{y} \quad \hat{z}]$ is the complex conjugate of a complex vector $[x \quad y \quad z]$, $Re(\alpha)$ represents the real part of a complex eigenvalue, $\alpha$ of $G$ and the corresponding non-zero eigenvector is defined as

$$(x, y, z) \neq (0, 0, 0)$$
$$x \in C^8 \, y \in C^1 \, z \in C^{20} \quad \text{(A8)}$$

we have

$$Re\left\{ \begin{bmatrix} \hat{x}^T & \hat{y}^T & \hat{z}^T \end{bmatrix} G \begin{bmatrix} x \\ y \\ z \end{bmatrix} \right\} = Re(\alpha)(x^2 + y^2 + z^2) \quad \text{(A9)}$$

The definition of $G$ in (A7)

$$Re\left\{ \begin{bmatrix} \hat{x}^T & \hat{y}^T & \hat{z}^T \end{bmatrix} G \begin{bmatrix} x \\ y \\ z \end{bmatrix} \right\}$$
$$= Re\left\{ \hat{x}^T \frac{\partial^2 L}{\partial u^2} x + \hat{x}^T \frac{\partial^2 L}{\partial u \partial \lambda} y + \hat{x}^T \frac{\partial^2 L}{\partial u \partial \eta} z - \hat{y}^T \frac{\partial^2 L}{\partial \lambda \partial u} x - \hat{z}^T \frac{\partial^2 L}{\partial \eta \partial u} x \right\}$$
$$= Re\left\{ \hat{x}^T \frac{\partial^2 L}{\partial u^2} x \right\} \quad \text{(A10)}$$

Then,

$$Re(\alpha)\left( ||x||^2 + ||y||^2 + ||z||^2 \right) = Re\left\{ \hat{x}^T \frac{\partial^2 L}{\partial u^2} x \right\} \quad \text{(A11)}$$

Since $\frac{\partial^2 L}{\partial u^2} > 0$, $Re(\alpha) > 0$,$G$ is strictly positive. Hence, $(u^*, \lambda^*, \eta^*)$ is asymptotically stable point of the adaptive control allocation system.

## Nomenclature

| | |
|---|---|
| $M_c$ | Yaw moment control signal (Nm) |
| $T_{mi}$ | Motor torque ($i = 1, 2, 3, 4$) (Nm) |
| $T_{mi\_max}$ | Max. motor torque ($i = 1, 2, 3, 4$) (Nm) |
| $T_{bi}$ | Tyre brake torque ($i = 1, 2, 3, 4$) (Nm) |
| $\delta_i$ | Tyre steering angle ($i = 1, 2, 3, 4$) (°) |
| $\delta_{i\_max}$ | Max. tyre steering angle ($i = 1, 2, 3, 4$) (°) |
| $\delta_{fc}$ | Front steering actuator command (°) |
| $\delta_{rc}$ | Rear steering actuator command (°) |
| $\delta_{driver}$ | Driver steering input (°) |
| $V_{cog}$ | Vehicle speed at centre of gravity (COG) (m/s) |
| $\beta$ | Vehicle side slip angle (°) |
| $r$ | Yaw rate (°/s) |
| $m$ | Vehicle mass (kg) |
| $F_{xi}$ | Longitudinal tyre force ($i = 1, 2, 3, 4$) (N) |
| $F_{yi}$ | Lateral tyre force ($i = 1, 2, 3, 4$) (N) |
| $I_z$ | Moment of inertia about $z$-axis (kgm$^2$) |
| $F_{xaero}$ | Aerodynamic force (N) |
| $\theta$ | Inclination angle (°) |
| $C_i$ | Cornering stiffness (N/rad) |
| $C_f$ | Front tyre cornering stiffness in single-track vehicle model (N/rad) |
| $C_r$ | Rear tyre cornering stiffness in single-track vehicle model (N/rad) |
| $R$ | Effective tyre radius (m) |
| $\omega_i$ | Tyre rotational speed ($i = 1, 2, 3, 4$) (rad/s) |
| $J_{\omega i}$ | Tyre moment of inertia ($i = 1, 2, 3, 4$) (kgm$^2$) |
| $\mu_i$ | Road friction coefficient ($i = 1, 2, 3, 4$) (–) |
| $l_f$ ($l_r$) | Distance from COG to front (rear axle) (m) |
| $t_1$ ($t_2$) | Distance from COG to left (right) track (m) |
| $d$ | Track width (m) |